*Supporting information*

# Distribution, chemical and molecular composition of high and low-molecular-weight humic-like substances in ambient aerosols

Xingjun Fan[a,b]*, Ao Cheng[a], Xufang Yu[a], Tao Cao[b,c], Dan Chen[a], Wenchao Ji[a], Yongbing Cai[a], Fande Meng[a], Jianzhong Song[b,]**, Ping'an Peng[b]

[a] College of Resource and Environment, Anhui Science and Technology University, Fengyang 233100, P. R. China

[b] State Key Laboratory of Organic Geochemistry, Guangzhou Institute of Geochemistry, Chinese Academy of Sciences, Guangzhou 510640, P. R. China

[c] University of Chinese Academy of Sciences, Beijing, 100049, PR China

* Corresponding authors

E-mail addresses: fanxj@ahstu.edu.cn (Xingjun Fan), songjzh@gig.ac.cn (Jianzhong Song)

**Text S1. Calculation of light absorption and fluorescence parameters.**

To characterize the optical and chemical properties of HULIS fractions, several parameters were calculated, including specific UV absorbance at 254 nm ($SUVA_{254}$), the UV absorbance ratio between 250 and 365 nm ($E_2/E_3$), spectra slope ratios ($S_R$), the absorption Angstrom exponent (AAE), and mass absorption efficiency ($MAE_{365}$), fluorescence indices (FI), biological index (BIX), and humification degree (HIX).

$SUVA_{254}$ represents the specific absorption at 254 nm, which is a measure of the aromaticity of organic matters (Kothawala et al., 2012; Williams et al., 2010). $E_2/E_3$ is the ratio of absorbance at 250 nm to that at 365 nm and indicates the relative abundance of aromatic structures in humic matters (Peuravuori and Pihlaja, 1997). $S_R$ is the spectral slope ratio calculated within specific wavelength ranges (275–295 nm and 350–400 nm) and provides information about the size and complexity of the organic matter (Helms et al., 2008).

$MAE_{365}$ and AAE (fitted within the wavelength range of 330-400 nm) are used to assess the light absorption efficiency and spectral dependence of the brown carbon, which were generally calculated using the following equations:

$$\mathrm{MAE}_{365} = \frac{A_{365}}{C \cdot l} \times \ln(10) \qquad ①$$

$$\mathrm{A}_{\lambda} = K \cdot \lambda^{-AAE} \qquad ②$$

where A is the absorbance, λ is the wavelength, C is the carbon content of HULIS, and $l$ is the optical length (0.01 m).

The fluorescence index (FI), biological index (BIX), and humification index (HIX) were calculated based on the EEM of the HULIS fractions. FI is calculated as the ratios of the fluorescence intensity at excitation and emission wavelengths (Ex/Em) of 370/470 nm to that at 370/520 nm (McKnight et al., 2001). BIX is calculated as the ratio of the intensity at Ex/Em of 310/380 nm to that at 310/430 nm (Huguet et al., 2009). HIX is calculated as the ratio of the intensity at wavelengths of 255/434−480 nm (average of the values on the line between 255/434 and 255/480 nm) to that at 255/300−344 nm (average of the values on the line between 255/300 and 255/344 nm) (Zsolnay et al., 1999). These indices provide insights into the composition and characteristics of the organic matter present in the HULIS fractions, particularly regarding their fluorescence properties and the degree of biological and humic transformation.

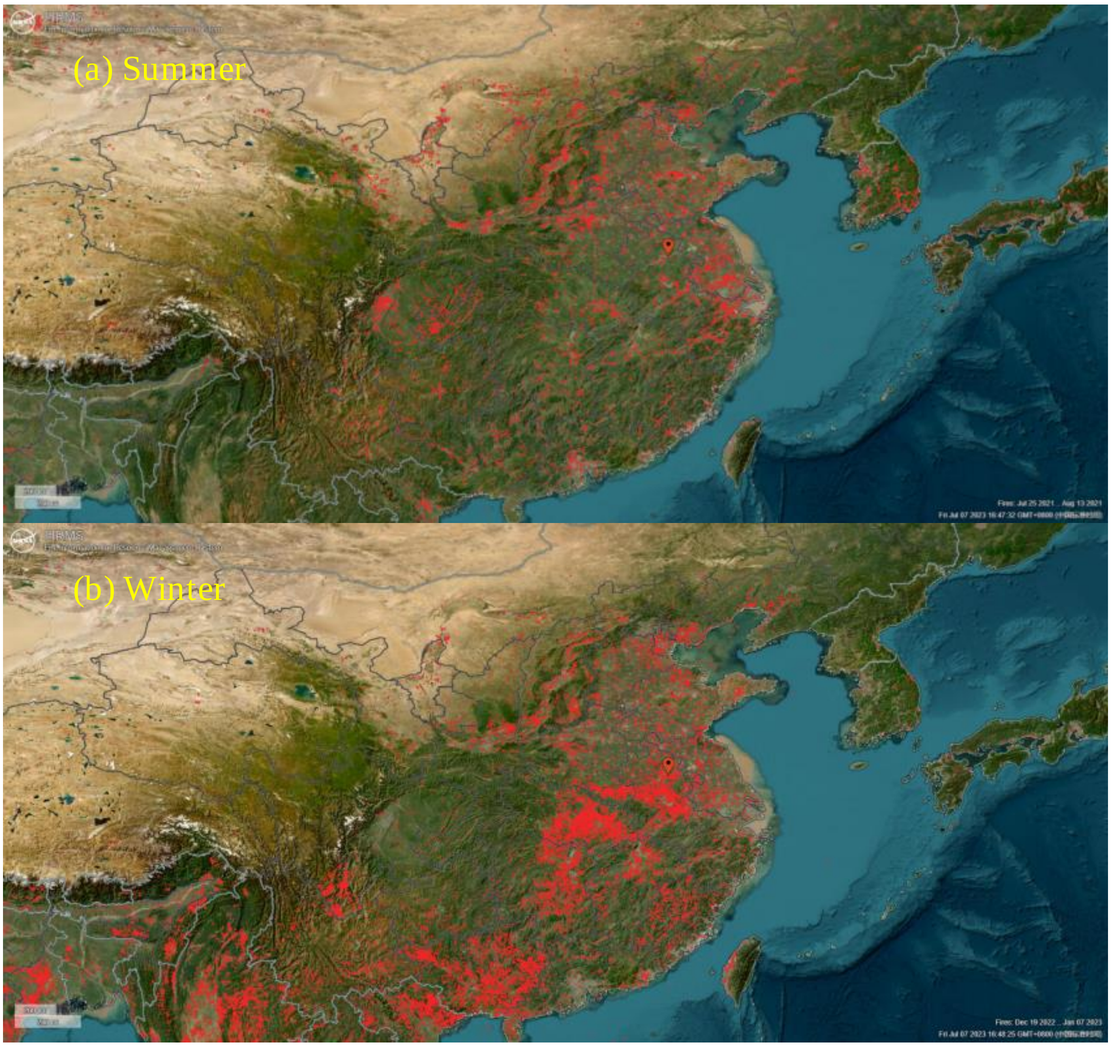


Fig. S1. The distribution of fire spots observed at sampling site during sampling period (https://firms.modaps.eosdis.nasa.gov/map/).

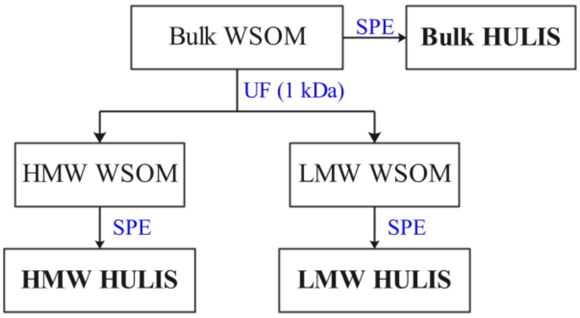


Fig. S2. Separation of size HULIS using ultrafiltration and solid phase extraction.

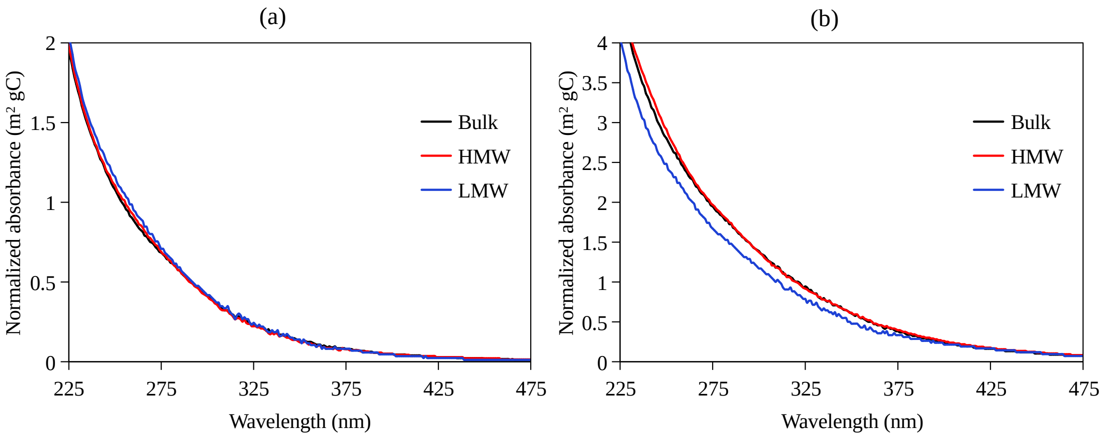


Fig. S3. The normalized UV-vis spectra with TOC of bulk, HMW and LMW HULIS from (a) summer and (b) winter aerosol samples.

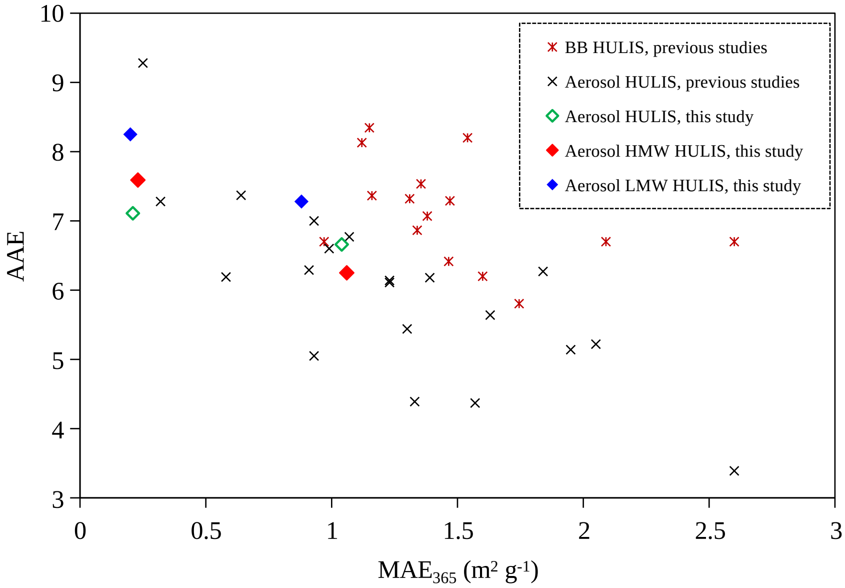


Fig. S4. Comparison of $MAE_{365}$ vs. AAE for HULIS fractions in ambient aerosols in this study to those of bulk HULIS reported in previous studies (Bao et al., 2022; Fan et al., 2018; Fan et al., 2016; Hong et al., 2022; Huo et al., 2018; Liu et al., 2018; Ma et al., 2019; Sun et al., 2021; Tang et al., 2020; Wu et al., 2018; Wu et al., 2020; Yuan et al., 2021; Zhang et al., 2022).

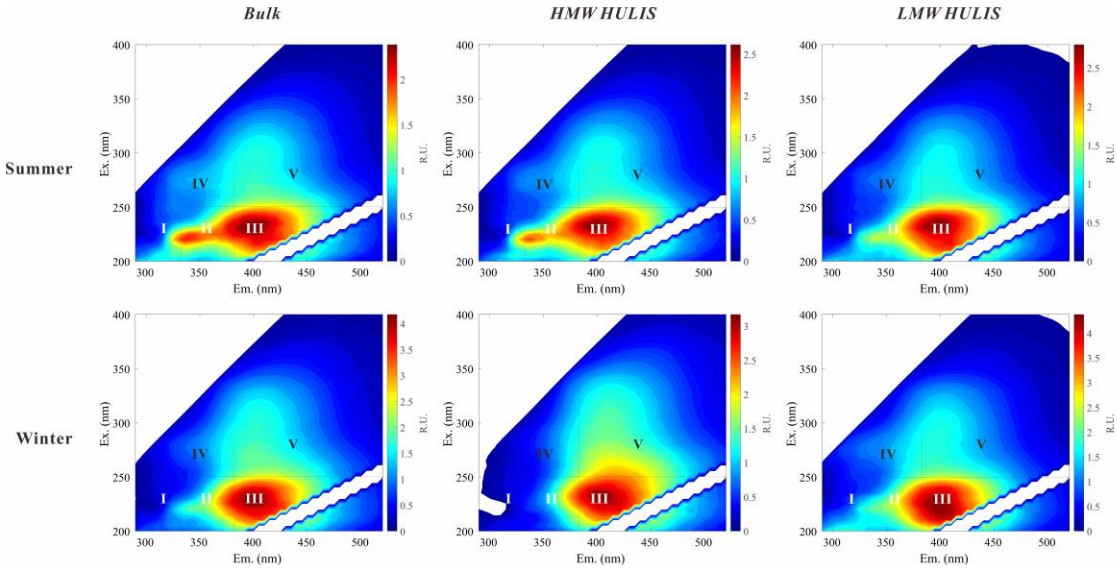


Fig. S5. Representative EEM contours of HMW and LMW HULIS from BB and ambient aerosols.

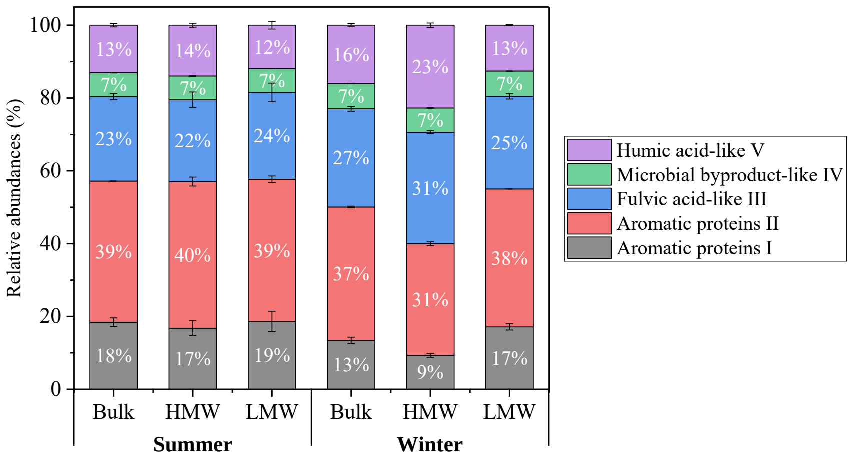


Fig. S6. The distributions of FRI-derived fluorophores within bulk and MW HULIS fractions in summer and winter aerosols.

Table S1. Concentrations of $NO_2$, $SO_2$ and $O_3$ at the sampling site during summer and winter.

| Date | $NO_2$ (μg $m^{-3}$) | $SO_2$ (μg $m^{-3}$) | $O_3$ (μg $m^{-3}$) |
|---|---|---|---|
| ***Summer*** | | | |
| 2021-07-25 | 7 | 10 | 80 |
| 2021-07-27 | 4 | 8 | 49 |
| 2021-07-29 | 5 | 9 | 73 |
| 2021-07-31 | 9 | 14 | 147 |
| 2021-08-02 | 14 | 14 | 136 |
| 2021-08-04 | 10 | 12 | 96 |
| 2021-08-06 | 12 | 13 | 108 |
| 2021-08-08 | 16 | 13 | 119 |
| 2021-08-10 | 20 | 14 | 178 |
| 2021-08-12 | 13 | 12 | 83 |
| Mean | 11.0 ± 5.0 | 11.9 ± 2.2 | 106.9 ± 38.8 |
| ***Winter*** | | | |
| 2021-12-19 | 40 | 13 | 70 |
| 2021-12-21 | 60 | 16 | 90 |
| 2021-12-23 | 57 | 11 | 80 |
| 2021-12-25 | 16 | 4 | 62 |
| 2021-12-27 | 45 | 12 | 63 |
| 2021-12-29 | 42 | 14 | 50 |
| 2021-12-31 | 60 | 18 | 71 |
| 2022-01-02 | 67 | 18 | 70 |
| 2022-01-04 | 45 | 11 | 87 |
| 2022-01-06 | 30 | 8 | 70 |
| Mean | 46.2 ± 15.5 | 12.5 ± 4.4 | 71.3 ± 12.0 |

Table S2. Compound classes identified by elemental ratios (H/C and O/C).

| Species | H/C | O/C |
|---|---|---|
| Lipids-like | 1.5<H/C≤2.0 | 0≤O/C≤0.3 |
| Protein/amino sugars | 1.5<H/C≤2.2 | 0.3<O/C≤0.67 |
| Carbohydrates | 1.5<H/C≤2.4 | 0.67<O/C≤1.2 |
| Unsaturated hydrocarbons | 0.7<H/C≤1.0 | 0<O/C<0.1 |
| Lignins | 0.7<H/C≤1.5 | 0.1≤O/C<0.67 |
| Condensed aromatics | 0.2≤H/C≤0.7 | 0<O/C<0.67 |
| Tannins | 0.5<H/C≤1.5 | 0.67<O/C≤1.2 |

Table S3. The average values of intensity-weighted molecular weights (MW), elemental ratios, double bond equivalents (DBE), modified aromaticity index (AImod) and carbon oxidation state (OSC) of unique categories of molecular compounds within each MW HULIS fractions.

| | | Categories of molecular compounds | MWw | H/Cw | O/Cw | N/Cw | S/Cw | O/Nw | O/Sw | OM/OCw | DBEw | DBE/Cw | DBE-Ow | AImod,w | OSCw |
|---|---|---|---|---|---|---|---|---|---|---|---|---|---|---|---|
| Summer | HMW HULIS | Lipids-like | 311 | 1.8 | 0.2 | 0.1 | 0.0 | 1.5 | 0.0 | 1.5 | 3.1 | 0.2 | -0.4 | 0.1 | -1.4 |
| | | Protein/amino sugars | 255 | 1.8 | 0.5 | 0.1 | 0.0 | 2.8 | 0.4 | 2.0 | 2.7 | 0.3 | -2.5 | 0.0 | -0.8 |
| | | Carbohydrates | 216 | 1.8 | 0.9 | 0.1 | 0.1 | 2.3 | 3.0 | 2.7 | 1.8 | 0.3 | -4.3 | 0.0 | 0.0 |
| | | Unsaturated hydrocarbons | 226 | 0.7 | 0.1 | 0.0 | 0.1 | 0.0 | 1.0 | 1.3 | 10.0 | 0.7 | 9.0 | 0.7 | -0.6 |
| | | Lignins | 255 | 1.2 | 0.4 | 0.1 | 0.0 | 2.0 | 0.2 | 1.9 | 6.0 | 0.5 | 1.3 | 0.5 | -0.4 |
| | | Condensed aromatics | 222 | 0.6 | 0.2 | 0.1 | 0.1 | 0.9 | 0.5 | 1.7 | 9.6 | 0.9 | 7.0 | 0.9 | -0.1 |
| | | Tannins | 228 | 1.2 | 0.8 | 0.3 | 0.1 | 2.9 | 2.4 | 2.7 | 4.9 | 0.7 | -1.1 | 0.3 | 0.5 |
| | LMW HULIS | Lipids-like | 467 | 1.7 | 0.2 | 0.0 | 0.0 | 5.3 | 5.3 | 1.6 | 4.8 | 0.2 | -1.0 | 0.0 | -1.3 |
| | | Protein/amino sugars | 344 | 1.7 | 0.6 | 0.0 | 0.1 | 0.1 | 5.3 | 2.0 | 3.2 | 0.2 | -4.5 | 0.0 | -0.6 |
| | | Carbohydrates | 308 | 1.7 | 0.8 | 0.0 | 0.1 | 1.2 | 7.1 | 2.5 | 2.7 | 0.3 | -5.6 | 0.0 | -0.1 |
| | | Unsaturated hydrocarbons | 0 | 0 | 0 | 0 | 0 | 0 | 0 | 0 | 0 | 0 | 0 | 0 | 0 |
| | | Lignins | 342 | 1.3 | 0.5 | 0.0 | 0.0 | 0.4 | 0.3 | 1.9 | 6.5 | 0.4 | -1.8 | 0.2 | -0.2 |
| | | Condensed aromatics | 192 | 0.6 | 0.6 | 0.0 | 0.0 | 0.0 | 0.3 | 1.9 | 7.1 | 0.9 | 2.0 | 0.9 | 0.6 |
| | | Tannins | 300 | 1.2 | 0.8 | 0.0 | 0.0 | 0.8 | 1.0 | 2.2 | 5.4 | 0.5 | -3.6 | 0.1 | 0.4 |
| Winter | HMW HULIS | Lipids-like | 314 | 1.8 | 0.2 | 0.1 | 0.1 | 1.6 | 0.2 | 1.6 | 3.0 | 0.2 | 0.2 | 0.0 | -1.5 |
| | | Protein/amino sugars | 208 | 1.8 | 0.5 | 0.1 | 0.0 | 0.8 | 0.5 | 2.0 | 2.1 | 0.3 | -2.4 | 0.0 | -0.7 |
| | | Carbohydrates | 215 | 2.0 | 0.9 | 0.1 | 0.0 | 1.9 | 0.0 | 2.4 | 1.3 | 0.2 | -5.3 | 0.0 | -0.2 |
| | | Unsaturated hydrocarbons | 0 | 0 | 0 | 0 | 0 | 0 | 0 | 0 | 0 | 0 | 0 | 0 | 0 |
| | | Lignins | 222 | 1.1 | 0.4 | 0.2 | 0.0 | 1.5 | 0.1 | 1.8 | 6.8 | 0.7 | 2.9 | 0.7 | -0.3 |
| | | Condensed aromatics | 219 | 0.6 | 0.3 | 0.0 | 0.0 | 1.3 | 0.1 | 1.5 | 9.6 | 0.8 | 6.1 | 0.8 | -0.1 |

| | | | | | | | | | | | | | | |
|---|---|---|---|---|---|---|---|---|---|---|---|---|---|---|
| | Tannins | 187 | 1.0 | 0.8 | 0.2 | 0.0 | 3.0 | 0.1 | 2.5 | 5.1 | 0.8 | -0.1 | 0.7 | 0.7 |
| LMW HULIS | Lipids-like | 308 | 1.7 | 0.2 | 0.1 | 0.0 | 0.9 | 0.3 | 1.6 | 4.5 | 0.3 | 1.5 | 0.1 | -1.3 |
| | Protein/amino sugars | 282 | 1.8 | 0.5 | 0.0 | 0.1 | 0.6 | 3.6 | 2.0 | 2.1 | 0.2 | -3.9 | 0.0 | -0.8 |
| | Carbohydrates | 270 | 1.8 | 0.8 | 0.0 | 0.1 | 2.6 | 7.1 | 2.6 | 2.0 | 0.2 | -5.2 | 0.0 | -0.2 |
| | Unsaturated hydrocarbons | 0 | 0 | 0 | 0 | 0 | 0 | 0 | 0 | 0 | 0 | 0 | 0 | 0 |
| | Lignins | 281 | 1.2 | 0.5 | 0.0 | 0.0 | 1.1 | 0.2 | 1.9 | 6.4 | 0.5 | 0.2 | 0.3 | -0.2 |
| | Condensed aromatics | 180 | 0.6 | 0.5 | 0.3 | 0.0 | 0.4 | 0.0 | 2.0 | 7.4 | 1.0 | 3.7 | 1.8 | 0.4 |
| | Tannins | 238 | 1.1 | 0.8 | 0.0 | 0.0 | 0.4 | 0.1 | 2.2 | 5.3 | 0.6 | -1.9 | 0.3 | 0.5 |

## References


Bao, M., Zhang, Y.-L., Cao, F., Lin, Y.-C., Hong, Y., Fan, M., Zhang, Y., Yang, X., Xie, F., 2022. Light absorption and source apportionment of water soluble humic-like substances (HULIS) in PM2.5 at Nanjing, China. Environmental Research 206, 112554.

Chen, Q., Hua, X., Dyussenova, A., 2021. Evolution of the chromophore aerosols and its driving factors in summertime Xi'an, Northwest China. Chemosphere 281, 130838.

Dey, S., Mukherjee, A., Polana, A.J., Rana, A., Mao, J., Jia, S., Yadav, A.K., Khillare, P.S., Sarkar, S., 2021. Brown carbon aerosols in the Indo-Gangetic Plain outflow: insights from excitation emission matrix (EEM) fluorescence spectroscopy. Environmental Science: Processes & Impacts 23, 745-755.

Fan, X., Cao, T., Yu, X., Wang, Y., Xiao, X., Li, F., Xie, Y., Ji, W., Song, J., Peng, P., 2020. The evolutionary behavior of chromophoric brown carbon during ozone aging of fine particles from biomass burning. Atmos. Chem. Phys. 20, 4593-4605.

Fan, X., Li, M., Cao, T., Cheng, C., Li, F., Xie, Y., Wei, S., Song, J., Peng, P.a., 2018. Optical properties and oxidative potential of water- and alkaline-soluble brown carbon in smoke particles emitted from laboratory simulated biomass burning. Atmos. Environ. 194, 48-57.

Fan, X., Wei, S., Zhu, M., Song, J., Peng, P., 2016. Comprehensive characterization of humic-like substances in smoke PM2.5 emitted from the combustion of biomass materials and fossil fuels. Atmos. Chem. Phys. 16, 13321-13340.

Fu, P., Kawamura, K., Chen, J., Qin, M., Ren, L., Sun, Y., Wang, Z., Barrie, L.A., Tachibana, E., Ding, A., Yamashita, Y., 2015. Fluorescent water-soluble organic aerosols in the High Arctic atmosphere. Sci Rep 5, 9845.

Hong, Y., Cao, F., Fan, M.-Y., Lin, Y.-C., Bao, M., Xue, Y., Wu, J., Yu, M., Wu, X., Zhang, Y.-L., 2022. Using machine learning to quantify sources of light-absorbing water-soluble humic-like substances (HULISws) in Northeast China. Atmos. Environ. 291, 119371.

Huo, Y., Li, M., Jiang, M., Qi, W., 2018. Light absorption properties of HULIS in primary particulate matter produced by crop straw combustion under different moisture contents and stacking modes. Atmos. Environ. 191, 490-499.

Liu, J., Mo, Y., Ding, P., Li, J., Shen, C., Zhang, G., 2018. Dual carbon isotopes (14C and 13C) and optical properties of WSOC and HULIS-C during winter in Guangzhou, China. Sci. Total Environ. 633, 1571-1578.

Ma, Y., Cheng, Y., Qiu, X., Cao, G., Kuang, B., Yu, J.Z., Hu, D., 2019. Optical properties, source apportionment and redox activity of humic-like substances (HULIS) in airborne fine particulates in Hong Kong. Environmental Pollution 255, 113087.

Qin, J., Zhang, L., Qin, Y., Shi, S., Li, J., Gao, Y., Tan, J., Wang, X., 2022. pH-Dependent Chemical Transformations of Humic-Like Substances and Further Cognitions Revealed by Optical Methods. Environ. Sci. Technol. 56, 7578-7587.

Qin, J., Zhang, L., Zhou, X., Duan, J., Mu, S., Xiao, K., Hu, J., Tan, J., 2018. Fluorescence fingerprinting properties for exploring water-soluble organic compounds in PM 2.5 in an industrial city of northwest China. Atmos. Environ. 184, 203-211.

Sun, H., Li, X., Zhu, C., Huo, Y., Zhu, Z., Wei, Y., Yao, L., Xiao, H., Chen, J., 2021. Molecular composition and optical property of humic-like substances (HULIS) in winter-time PM2.5 in the rural area of North China Plain. Atmos. Environ. 252, 118316.

Tang, J., Li, J., Mo, Y., Safaei Khorram, M., Chen, Y., Tang, J., Zhang, Y., Song, J., Zhang, G., 2020. Light absorption and emissions inventory of humic-like substances from simulated rainforest biomass burning in Southeast Asia. Environmental Pollution 262, 114266.

Wu, G., Wan, X., Gao, S., Fu, P., Yin, Y., Li, G., Zhang, G., Kang, S., Ram, K., Cong, Z., 2018. Humic-Like Substances (HULIS) in Aerosols of Central Tibetan Plateau (Nam Co, 4730 m asl): Abundance, Light Absorption Properties, and Sources. Environ. Sci. Technol. 52, 7203-7211.

Wu, G., Wan, X., Ram, K., Li, P., Liu, B., Yin, Y., Fu, P., Loewen, M., Gao, S., Kang, S., Kawamura, K., Wang, Y., Cong, Z., 2020. Light absorption, fluorescence properties and sources of brown carbon aerosols in the Southeast Tibetan Plateau. Environmental Pollution 257, 113616.

Xie, M., Mladenov, N., Williams, M.W., Neff, J.C., Wasswa, J., Hannigan, M.P., 2016. Water soluble organic aerosols in the Colorado Rocky Mountains, USA: composition, sources and optical properties. Scientific Reports 6, 39339.

Xie, X., Chen, Y., Nie, D., Liu, Y., Liu, Y., Lei, R., Zhao, X., Li, H., Ge, X., 2020. Light-absorbing and fluorescent properties of atmospheric brown carbon: A case study in Nanjing, China. Chemosphere 251, 126350.

Yuan, W., Huang, R.-J., Yang, L., Ni, H., Wang, T., Cao, W., Duan, J., Guo, J., Huang, H., Hoffmann, T., 2021. Concentrations, optical properties and sources of humic-like substances (HULIS) in fine particulate matter in Xi'an, Northwest China. Sci. Total Environ. 789, 147902.

Yue, S., Ren, L., Song, T., Li, L., Xie, Q., Li, W., Kang, M., Zhao, W., Wei, L., Ren, H., Sun, Y., Wang, Z., Ellam, R.M., Liu, C.-Q., Kawamura, K., Fu, P., 2019. Abundance and Diurnal Trends of Fluorescent Bioaerosols in the Troposphere over Mt. Tai, China, in Spring. Journal of Geophysical Research: Atmospheres 124, 4158-4173.

Zhang, T., Huang, S., Wang, D., Sun, J., Zhang, Q., Xu, H., Hang Ho, S.S., Cao, J., Shen, Z., 2022. Seasonal and diurnal variation of PM2.5 HULIS over Xi'an in Northwest China: Optical properties, chemical functional group, and relationship with reactive oxygen species (ROS). Atmos. Environ. 268, 118782.